Transport and stability of long-pulse relativistic electron beams in UV laser-induced ion channels

R. F. Lucey, Jr.,[a] R. M. Gilgenbach, J. D. Miller, J. E. Tucker, and R. A. Bosch
Intense Energy Beam Interaction Laboratory, Nuclear Engineering Department, The University of Michigan, Ann Arbor, Michigan 48109-2104

(Received 3 May 1988; accepted 7 October 1988)

Results are presented for the first experiments in which long-pulse (0.4–1 μsec), relativistic (0.8 MV) electron beams have been transported in the ion focused regime (IFR) in ion channels formed in low pressure diethylaniline gas by means of KrF excimer laser-induced ionization. These experiments demonstrate that the most efficient (50%–80%) and longest pulse (0.6 μsec) *e*-beam transport is obtained with laser-induced channels over a very narrow gas pressure range (0.3–1.7 mTorr). Higher than optimal pressures cause excess *e*-beam induced ionization and instability of the electron beam. At lower pressures, the laser-induced ion channel density is insufficient for initial *e*-beam guidance. Transverse oscillations of the electron beam have been measured at a frequency close to that predicted for the ion hose instability. The growth length and wavelength of the transverse oscillations are comparable to the betatron wavelength, further suggesting that these oscillations result from the ion hose instability.

I. INTRODUCTION

Intense, relativistic electron beams with microsecond pulse lengths have significant applications to free electron lasers,[1,2] cyclotron masers,[3] and plasma heating.[4] In recent years, several research groups have demonstrated efficient transport[5–7] and stabilization[7] of short pulses (much less than 100 nsec) and pulse trains[5] in laser-induced ion channels. Those experiments have relied upon ion focused regime (IFR) transport in which the channel ion density is chosen to compensate the electron beam space charge repulsion and transverse pressure to permit *e*-beam propagation in a self-pinched mode. For an electron beam with a Bennett profile, the required condition for IFR focusing is

$$f_e \geq 1/\gamma^2 + 2T_\perp/\nu mc^2, \qquad (1)$$

where f_e is the space charge neutralization fraction, γ is the relativistic factor, m is electron mass, c is the speed of light, ν is Budker's parameter, and $T_\perp$ is the transverse temperature of the electron beam. The first term represents compensation of the *e*-beam space charge repulsion while the second term is an electron pressure term. The space charge term dominates when the electron Debye length in the beam frame is much less than the beam diameter.[8]

An important area of research concerns the transport efficiency and stability of ion-focused-regime propagation over longer time scales, on the order of 1 μsec. Other experiments[9,10] have studied the transport of long-pulse (greater than 100 nsec) *e* beams in either self-ionized[9] or low energy *e*-beam induced[10] ion channels. The experiments reported here represent the first investigation of long-pulse (0.4–1 μsec) electron beam transport in excimer-laser-induced ion channels.[11]

[a] Present address: Massachusetts Institute of Technology Lincoln Laboratories, Lexington, Massachusetts 02173-0073.

II. EXPERIMENTAL CONFIGURATION

Electron beams were generated by the Michigan Electron Long Beam Accelerator (MELBA), which operates with parameters of voltage = -0.7 to -1 MV, diode current = 1–30 kA, and a pulse length, which is adjustable by a crowbar switch from 0.3–1.5 μsec. This accelerator consists of a modified Marx generator, in which the voltage is compensated by a reverse-charged resistance–inductance–capacitance (RLC) ringing circuit; further details on the generator are given in Ref. 12. The experimental configuration is depicted in Fig. 1. Two types of cold cathode were employed in these studies: (1) cotton velvet recessed in a metallic shield, and (2) carbon brush on a bare aluminum plate. More details of the cathodes are given in Refs. 11 and 12. The electron beam anode for these experiments was a graphite plate with a 2.54 cm diam aperture for *e*-beam extraction. The anode cathode (A–K) gap was typically 6.9 cm for the velvet cathode and 8 cm for the brush cathode. These configurations gave an injected electron beam current of 200–300 A with an *e*-beam diameter of 2.54 cm. The diode vacuum ($< 10^{-4}$ Torr) region was separated from the interaction chamber gas by a 6.3 μm thick aluminized Mylar foil. These foils withstood several crowbarred generator pulses before pinholes formed.

The electron beam was injected through the anode foil into a lead-covered, stainless steel interaction chamber of length 1.2 m and maximum diameter 0.75 m. This chamber was evacuated by a turbomolecular pump to 6×10^{-6} Torr before continuously leaking in diethylaniline (DEA) vapor, which was generated by heating DEA in an external flask. The DEA was chosen since it has been shown[13] to have a high cross section for ionization by KrF excimer laser radiation at 249 nm.

The excimer laser was a Lumonics TE-292 K, which generated about 1 J in a 25 nsec FWHM pulse. The laser beam was collimated by a 2.4 cm diam aperture before the

 0699-8221/89/020430-05$01.90

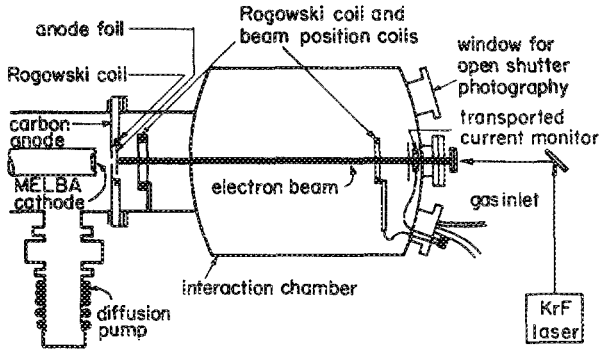

FIG. 1. Experimental configuration for long-pulse REB propagation in laser preionized channels.

quartz input window in order to match approximately the diameter of the laser-induced ion channel to the e-beam diameter. After losses and divergence, the laser had a peak fluence in the chamber of about 10 mJ/cm^2. Charge collection plate measurements have shown that the laser-induced ion channel density can be controlled up to about 10^{10} cm^{-3}; lower ion densities were obtained by either attenuating the laser beam with thin plastic sheets or lowering the DEA pressure. It should be noted that in ion channel experiments utilizing DEA (150 amu), there exists some uncertainty as to the actual ion masses that exist after UV laser and electron beam irradiation.

A number of e-beam diagnostics have been employed to measure the current and centroid position of the electron beam. The injected e-beam current was measured by a Rogowski coil located in the anode flange just after the anode foil (defined as $z = 0$). Two sets of X–Y beam centroid position sensing probes were employed, one at $z = 14$ cm (upstream X–Y) and another at $z = 95$ cm (downstream X–Y). These beam centroid position probes consisted of an array of four identical magnetic loops rigidly mounted to, but electrically isolated from, a 0.3 cm thick brass plate. This plate had a 20 cm outside diameter and a 7.6 cm diam aperture through which the beam could pass. The choice of the aperture size was based on the need to have reasonable signal and linear response from the position probes for beam displacements of several centimeters. The brass plate was positioned facing the diode to stop electrons that did not pass through the aperture. The backside of the probe was covered by a 0.12 mm stainless steel foil. A 0.12 mm stainless steel foil formed a cylinder defining the 7.6 cm diam aperture through which the electron beam passed and shielded the coils from electrons that were lost radially. The shielding also discriminated against the high levels of rf radiation associated with beam–plasma interactions. The four coils were spaced equally around the aperture, oriented to detect the B_θ component of the magnetic field produced by the electron beam. The signals from diametrically opposing coils were electrically integrated and subtracted to give a signal proportional to the net current and the beam centroid displacement. A Rogowski coil built into the same brass housing (at $z = 95$ cm) measured the net current passing through the aperture.

In laser guiding experiments, the transported electron beam current was measured (at $z = 112$ cm) with a Pearson current transformer in which the 5 cm diam aperture was covered by thin (25 μm) plastic to exclude plasma current, but allow the excimer laser light and the high energy electron beam to pass through. An x-ray pinhole camera imaged the footprint of the transported beam on the (3.5 cm diam) quartz laser input window. Open shutter visible photography was performed through the upper port on the downstream end of the chamber. The time integrated transverse position of the propagating electron beam was visible from fluorescence when the beam passed through a grid of thin nylon filaments.

III. EXPERIMENTAL RESULTS

In these experiments, as much as 10 mJ/cm^2 of excimer-laser radiation ionized DEA gas 200 nsec prior to the voltage rise of the electron beam. For the pressures and laser energies that gave electron beam propagation in preionized channels, values of f_e at the beginning of electron beam injection were between 0.3 and 0.9. These values should be compared to $1/\gamma^2 = 0.16$ for the electron beam and indicate that the electron beam was initially injected into an ion focused regime channel. Later in the pulse, $f_e = 1$ can be exceeded as a result of e-beam induced ionization of the DEA.[14]

Diagnostic signals for electron beam transport in a laser-induced ion channel are presented in Fig. 2 for an injected e-beam pulse width of about 1 μsec and a DEA pressure of 0.57 mTorr. Examination of the diagnostic data in Fig. 2 shows the following effects.

(1) The transported e-beam current initially starts at about 50% of the injected e-beam current (I_{ei}) and increases during the pulse to about 60% of I_{ei} before rapidly decreasing to zero at 0.6 μsec into the pulse.

(2) The net current is nearly equal to the injected e-beam current (zero plasma current) from 0.1–0.4 μsec after the current rise. The net current gradually decreases until it passes through zero 0.63 μsec after the start of the e-beam current. (Recall that the conventional notation is: $\mathbf{J}_{\text{beam}} + \mathbf{J}_{\text{plasma}} = \mathbf{J}_{\text{net}}$.)

(3) A spike in the injected e-beam current is accompanied by a large net current reversal and a small negative spike in the transported current monitor.

(4) Transverse oscillations occur in the downstream beam centroid position monitors with a magnitude of about $\pm$ 1 cm and a period of about 0.6 μsec during the duration of beam propagation.

By operating at a slightly higher pressure of 1.7 mTorr (Fig. 3) with laser-induced preionization it was possible to transport between 50% and 80% of the injected current during the first 0.25 μsec. In this case, the downstream transverse beam oscillations (of about $\pm$ 1.3 cm) grow more rapidly (0.4 μsec period) and beam transport through the downstream ($z = 95$ cm) position coils and Rogowski persists for 0.4 μsec. Transport to the end of the chamber decreased to zero after about 0.28 μsec.

In Fig. 4 we plot the X vs Y beam centroid displacement as a function of time for the data of Figs. 2(d) and 2(e). It can be seen that the beam undergoes an oscillation near the axis before undergoing a large, rapid excursion away from the axis near the end of the transported pulse.

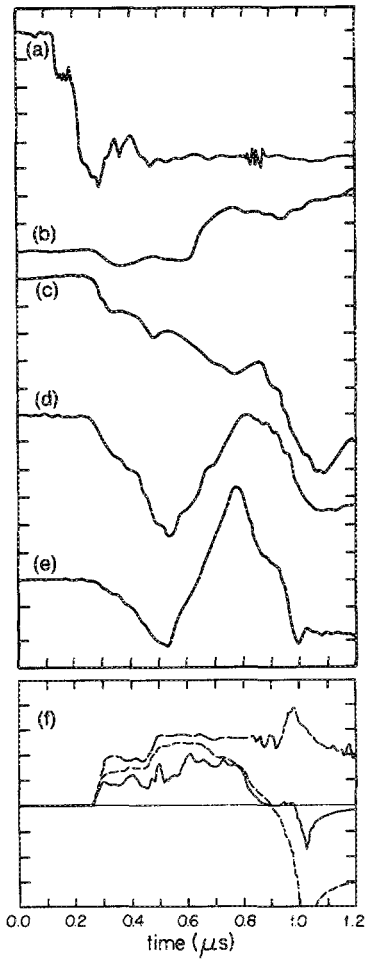

FIG. 2. Experimental data for electron beam injection into laser preionized channels in DEA at 0.57 mTorr: (a) voltage (155 kV/div); (b) upstream X position of e-beam centroid ($z = 14$ cm, 0.1 kA cm/div); (c) upstream Y position of e-beam centroid ($z = 14$ cm, 0.1 kA cm/div); (d) downstream X position of e-beam centroid ($z = 95$ cm, 0.1 kA cm/div); (e) downstream Y position of e-beam centroid ($z = 95$ cm, 0.1 kA cm/div); (f) injected current (long dashed line), net current (short dashed line) at 95 cm, and transported current (solid line) at 112 cm, 100 A/div (velvet cathode).

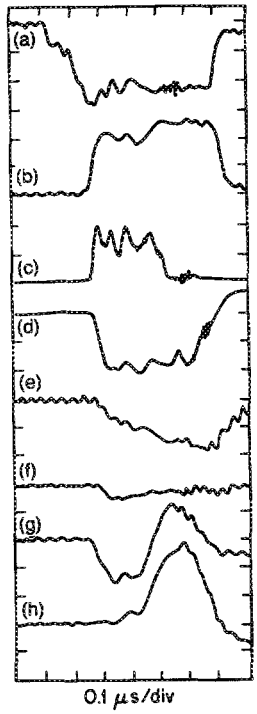

FIG. 3. Experimental data for electron beam injection into laser preionized channels in DEA at 1.7 mTorr: (a) voltage (310 kV/div); (b) injected current (112 A/div); (c) transported current 112 cm from anode (100 A/div); (d) net current 95 cm from anode ($-$ 75 A/div); (e) upstream X position of e-beam centroid position ($z = 14$ cm, 0.2 kA cm/div); (f) upstream Y position of e-beam centroid ($z = 14$ cm, 0.2 kA cm/div); (g) downstream X position of e-beam centroid ($z = 95$ cm, 0.2 kA cm/div); (h) downstream Y position of e-beam centroid ($z = 95$ cm, 0.2 kA cm/div) (velvet cathode).

The temporal dependence of laser guided electron beam current transport at three different DEA pressures is depicted in Fig. 5 for an injected current of about 220 A over a 0.5 μsec pulse length. For the laser intensities employed in these experiments, a narrow pressure window existed for efficient electron beam transport. When the pressure was too low (0.3 mTorr), the transport was inefficient until e-beam induced ionization was sufficient to give ion focused conditions after about 0.4 μsec. At the high pressure edge (1.7 mTorr) of the propagation window, beam transport was initially efficient (80%), but propagation was cut off after e-beam instability ejected the beam from the channel after about 0.26 μsec. The optimal DEA pressure for laser guided transport in these experiments was about 0.4–0.7 mTorr, for which 50%–60% e-beam transport was observed for pulse lengths up to about 0.6 μsec.

Laser guided e-beam propagation data is summarized and compared with neutral gas transport in Fig. 6. Several features are notable in this figure. First, the optimal pressure window for efficient laser guided propagation is apparent. Second, laser guided propagation showed higher peak transported charge using the velvet cathode over the brush cathode, but this is mainly due to lower injected current and shorter pulse lengths with the brush cathode. The superior performance of the velvet cathode was caused by a much lower rate of cathode plasma diode closure, which permitted longer pulses. Third, laser guided propagation in DEA transported a factor of 2.5 times more energy (and charge) than the highest efficiency propagation data obtained in these experiments in neutral air.

An open shutter photograph of the light emitted by a laser guided electron beam propagating through DEA and a

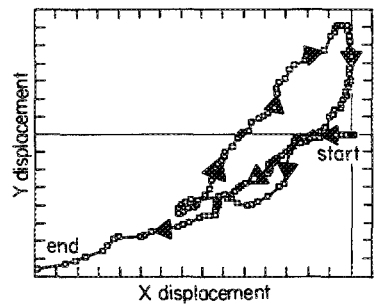

FIG. 4. Trajectory of e-beam centroid for data of Figs. 2(d) and 2(e) as a function of time at $z = 95$ cm. The data points are spaced by 6 nsec (0.05 kA cm/div).

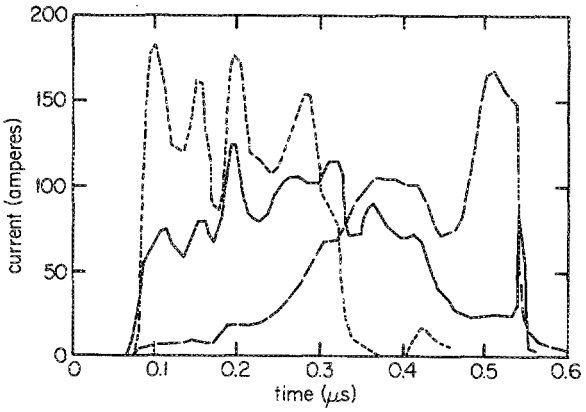

FIG. 5. Temporal evolution of laser guided electron beam current over several DEA pressures within the propagation window. Solid line: 0.46 mTorr, short dashed line: 1.7 mTorr, long dashed line: 0.31 mTorr (velvet cathode).

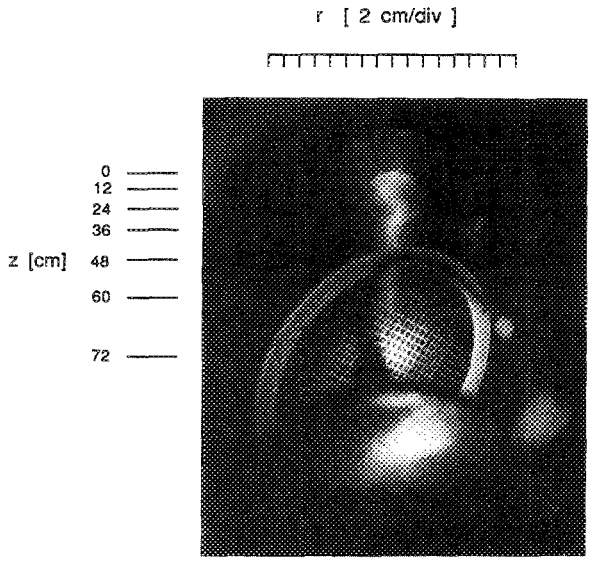

FIG. 7. Open shutter photograph of laser guided electron beam transport through a grid of thin nylon filaments that has been viewed from the upper port at the end of the tank with DEA pressure of 0.7 mTorr.

nylon grid is presented in Fig. 7. (It should be noted that the laser alone gave no visible emission except for weak fluorescence of the nylon grid.) The relatively large illuminated area on the nylon grid indicates significant transverse motion of the e beam. This pulse gave the most apparent photographic evidence of hose structure. The wavelength of this hose structure is about 25 cm.

A 1.8–2.1 cm diam x-ray image was measured where the e beam struck the laser input window at the end of the chamber. An x-ray image was only obtained when the other diagnostics showed effective e-beam transport from laser guiding.

IV. DISCUSSION AND ANALYSIS

Ion focused regime propagation of long-pulse electron beams in laser-induced ion channels has been demonstrated in these experiments over a narrow range of DEA pressure. The observations of the low pressure limit on IFR propagation when $f_e \geqslant 0.3 \approx 2/\gamma^2$ suggests that the beam transverse pressure forces are comparable to electrostatic repulsion forces.[8]

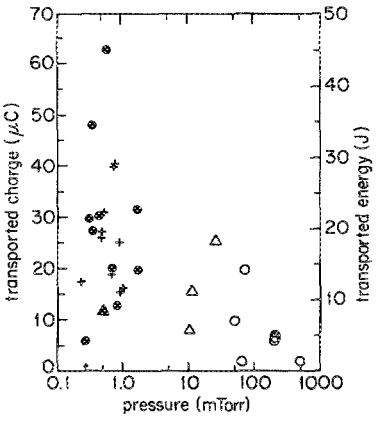

FIG. 6. Summary of transported charge and energy for laser guided e-beam transport and neutral gas e-beam transport. Here, ●: DEA for laser preionized channels with velvet cathode; + DEA for laser preionized channels with brush cathode; ▲: neutral DEA gas with velvet cathode; ○: neutral helium with velvet cathode; △: neutral air with velvet cathode.

For the DEA pressures employed in these experiments, electron beam-induced ionization (Δn_i) can be significant since

$$\Delta n_i / n_e = \sigma n_g v t, \tag{2}$$

where σ is the cross section for DEA of about 5×10^{-18} cm^2, n_g is DEA gas density, v is the e-beam velocity, and t is the time after the start of the injected current. Thus in the lower pressure range (0.3 mTorr) for laser guiding

$$\Delta n_i / n_e \approx 1$$

after 0.7 μsec. Since f_e $(t=0) \cong 0.3$ for laser guiding at 0.3 mTorr, then $f_e = 1$ is exceeded at about 0.5 μsec. At the optimal pressures ($\sim$0.7 mTorr) studied with laser guiding,

$$\Delta n_i / n_e \approx 1$$

after about 0.3 μsec. At the upper pressure propagation limit in these experiments, e-beam induced DEA ionization can cause $f_e > 1$ very early in the beam pulse, after about 0.1 μsec. Since laser-induced ionization sets the initial $f_e \approx 0.9$ in the high pressure case, $f_e > 1$ should occur early (about 0.01 μsec) in the pulse, during the current rise. Excess ionization from $f_e > 1$ could lead to electron–electron streaming instabilities that could disrupt propagation.[15]

The experimental data of Figs. 2 and 3 show transverse oscillations of the electron beam. In Figs. 2(d) and 2(e), at 0.57 mTorr, the experimentally observed frequency is about 1.7 MHz for the maximum excursion of transverse oscillation on the downstream beam centroid position monitor. A theory of the ion hose instability[8] predicts the oscillation frequency of

$$\frac{\omega_{pi}}{2\pi\sqrt{2f_e}} = \frac{1}{2\pi\sqrt{2}}\left(\frac{n_e e^2}{\epsilon_0 m_i}\right)^{1/2}, \tag{3}$$

which is estimated to be about 1.3 MHz. This is in good agreement within the experimental uncertainty, suggesting

that the transverse oscillations arise from the ion hose instability. The hose oscillation frequency of Fig. 3(g) is about 2.5 MHz. This is consistent with a factor of 3 increase in the e-beam density, expected to result from contraction of the beam when injected into a channel with $f_e = 0.9$ when the low pressure limit for IFR propagation is $f_e = 0.3$. The x-ray pinhole photography data showed a propagating e-beam diameter of 1.8–2.1 cm, compared with channel and injected e-beam diameters of 2.4 and 2.54 cm, respectively. This corresponds to an increase in the e-beam density in the range 1.5–2. The observation of hose oscillation frequencies that are slightly higher than the theoretical value is possible if the average ion mass was lower than the molecular weight of DEA. This could occur if the laser and e-beam irradiation caused splitting of the DEA molecules.

The observation of significant transverse oscillation after about 1 m of propagation suggests the growth of the instability in a propagation length on the order of one betatron wavelength (40 cm at the center of the beam or a beam average betatron wavelength of 80 cm). This observed growth length is consistent with theoretical predictions for the ion hose instability.[8,16] The existence of hose oscillations is further suggested by open shutter photography data in Fig. 7. Other researchers[17] have noted that light emission from e-beam channel interactions is expected to occur mainly after $f_e > 1$. This light could originate from a return current that flows along the e-beam ionized path after $f_e = 1$ is exceeded.

V. SUMMARY

Ion focused regime propagation of a long-pulse electron beam in a laser-induced ion channel has been observed. The pressure limits (0.3–1.7 mTorr) for propagation suggest that efficient propagation occurred when $f_e > 2/\gamma^2$, consistent with expectations for a warm e beam; loss of transport occurred at the higher pressures for which $f_e \gg 1$. Observations of transverse beam oscillations with time scales on the order of the ion plasma period of the channel as well as a visible hose structure are strong evidence of the ion hose instability.

ACKNOWLEDGMENTS

We appreciate the comments of the referee, which improved this paper. This research was supported by the Office of Naval Research, National Science Foundation Grant No. ECS-8351837, and SDIO-IST.

[1] T. C. Marshall, *Free-Electron Lasers* (Macmillan, New York, 1985).

[2] J. A. Pasour, R. F. Lucey, and C. W. Roberson, in *Free-Electron Generators of Coherent Radiation* (SPIE, Bellingham, WA, 1983), Vol. 453, p. 328; C. W. Roberson, J. Pasour, F. Mako, R. F. Lucey, Jr., and P. Sprangle, in *Infrared and Millimeter Waves*, edited by K. J. Button (Academic, New York, 1982), Vol. 10, p. 361.

[3] R. M. Gilgenbach, R. A. Bosch, J. Choi, and J. G. Wang, in *Conference Digest of the Twelfth International Conference on Infrared and Millimeter Waves* (IEEE, New York, 1987), p. 282.

[4] C. W. Roberson, Nucl. Fusion **18**, 1693 (1978).

[5] R. L. Carlson, S. W. Downey, and D. C. Moir, J. Appl. Phys. **61**, 12 (1987).

[6] S. L. Shope, C. A. Frost, G. T. Leifeste, and J. W. Poukey, Phys. Rev. Lett. **58**, 551 (1987).

[7] G. J. Caporaso, F. Rainer, W. E. Martin, D. S. Prono, and A. G. Cole, Phys. Rev. Lett. **57**, 1591 (1986); W. E. Martin, G. J. Caporaso, W. M. Fawley, D. Prosnitz, and A. G. Cole, *ibid.* **54**, 685 (1985).

[8] R. A. Bosch and R. M. Gilgenbach, Phys. Fluids **31**, 634 (1988).

[9] J. R. Smith, R. F. Schneider, M. J. Rhee, H. S. Uhm, and W. Namkung, J. Appl. Phys. **60**, 4119 (1986); R. F. Schneider and J. R. Smith, Phys. Fluids **29**, 3917 (1986); K. T. Nguyen, R. F. Schneider, J. R. Smith, and H. S. Uhm, Appl. Phys. Lett. **50**, 239 (1987).

[10] T. R. Lockner, G. W. Kamin, J. S. Wagner, K. J. O'Brien, I. R. Shokair, R. J. Lipinski, P. D. Kiekel, I. Molina, D. J. Armistead, S. R. Hogeland, and E. T. Powell, Bull. Am. Phys. Soc. **32**, 1868 (1987); K. J. O'Brien, G. W. Kamin, T. R. Lockner, J. S. Wagner, I. R. Shokair, P. D. Kiekel, I. Molina, J. J. Armistead, S. Hogeland, E. T. Powell, and R. J. Lipinski, Phys. Rev. Lett. **60**, 1278 (1988).

[11] R. F. Lucey, Jr., Ph.D. dissertation, The University of Michigan, 1988; also, R. M. Gilgenbach, R. F. Lucey, L. D. Horton, M. L. Brake, S. Bidwell, M. Cuneo, J. D. Miller, and L. Smutek, Bull. Am. Phys. Soc. **30**, 1502 (1985).

[12] R. M. Gilgenbach, L. D. Horton, R. F. Lucey, Jr., S. Bidwell, M. Cuneo, J. Miller, and L. Smutek, in *Proceedings of the 5th IEEE Pulsed Power Conference* (IEEE, New York, 1985), p. 126; see also, M. E. Cuneo, R. M. Gilgenbach, and M. L. Brake, IEEE Trans. Plasma Sci. **PS-15**, 375 (1987).

[13] J. R. Woodworth, T. A. Green, and C. A. Frost, J. Appl. Phys. **57**, 1648 (1985).

[14] F. F. Rieke, F. Foster, and W. Prepejchal, Phys. Rev. A **6**, 1507 (1972).

[15] Y. Y. Lau (private communication).

[16] H. L. Buchanon, Phys. Fluids **30**, 221 (1987).

[17] T. R. Lockner (private communication).